

Cationic (fluoromesityl)palladium(II) complexes

Camino Bartolomé, Raquel de Blas, Pablo Espinet*, Jose Miguel Martín-Alvarez,
Fernando Villafañe

Química Inorgánica, Facultad de Ciencias, Universidad de Valladolid, 47005 Valladolid, Spain

Received 20 April 2006; received in revised form 18 May 2006; accepted 18 May 2006
Available online 3 June 2006

Warmly dedicated to Professor Antonio Abad on occasion of his premature retirement.

Abstract

Halide abstraction from $[\text{Pd}(\mu\text{-Cl})(\text{Fmes})(\text{NCMe})_2]$ (Fmes = 2,4,6-tris(trifluoromethyl)phenyl or nonafluoromesityl) with TIBF_4 in $\text{CH}_2\text{Cl}_2/\text{MeCN}$ gives $[\text{Pd}(\text{Fmes})(\text{NCMe})_3]\text{BF}_4$, which reacts with monodentate ligands to give the monosubstituted products *trans*- $[\text{Pd}(\text{Fmes})\text{L}(\text{NCMe})_2]\text{BF}_4$ (L = PPh_3 , $\text{P}(o\text{-Tol})_3$, 3,5-lut, 2,4-lut, 2,6-lut; lut = dimethylpyridine), the disubstituted products *trans*- $[\text{Pd}(\text{Fmes})(\text{NCMe})(\text{PPh}_3)_2]\text{BF}_4$, *cis*- $[\text{Pd}(\text{Fmes})(3,5\text{-lut})_2(\text{NCMe})]\text{BF}_4$, or the trisubstituted products $[\text{Pd}(\text{Fmes})\text{L}_3]\text{BF}_4$ (L = CN^tBu , PPh_2 , 3,5-lut, 2,4-lut). Similar reactions using bidentate chelating ligands give $[\text{Pd}(\text{Fmes})(\text{L-L})(\text{NCMe})]\text{BF}_4$ (L-L = bipy, tmeda, dppe, $\text{OPPhPy}_2\text{-}N,N'$, $(\text{OH})(\text{CH}_3\text{CPy}_2\text{-}N,N')$). The complexes *trans*- $[\text{Pd}(\text{Fmes})\text{L}_2(\text{NCMe})]\text{BF}_4$ (L = PPh_3 , tht) (tht = tetrahydrothiophene) and $[\text{Pd}(\text{Fmes})(\text{L-L})(\text{NCMe})]\text{BF}_4$ (L-L = bipy, tmeda) were obtained by halide extraction with TIBF_4 in $\text{CH}_2\text{Cl}_2/\text{MeCN}$ from the corresponding neutral halogeno complexes *trans*- $[\text{Pd}(\text{Fmes})\text{ClL}_2]$ or $[\text{Pd}(\text{Fmes})\text{Cl}(\text{L-L})]$. The aqua complex *trans*- $[\text{Pd}(\text{Fmes})(\text{OH}_2)(\text{tht})_2]\text{BF}_4$ was isolated from the corresponding acetonitrile complex. Overall, the experimental results on these substitution reactions involving bulky ligands suggest that thermodynamic and kinetic steric effects can prevail affording products or intermediates different from those expected on purely electronic considerations. Thus, water, whether added on purpose or adventitious in the solvent, frequently replaces in part other better donor ligands, suggesting that the smaller congestion with water compensates for the smaller M–OH₂ bond energy. © 2006 Elsevier B.V. All rights reserved.

Keywords: Palladium; Fluoromesityl; Steric effects; Kinetic; Aqua; Cationic

1. Introduction

The bulky ligand 2,4,6-tris(trifluoromethyl)phenyl (nonafluoromesityl or Fmes) gives rise to interesting structural features when coordinated to main group [1], or to transition metals [2], due to its high steric requirements combined with a certain electron withdrawing character. Its coordination to palladium has led to some unusual complexes, such as an unprecedented self-assembled pyramidal tetrametallic complex with a halide in the apex in complexes $[\text{Pd}_4(\text{Fmes})_4\text{X}_5]^-$ (X = Cl, Br, I), a number of neutral aqua complexes, or the formation of a new halocarbon ligand acting as halo-donor chelate [3]. Herein we report the synthesis of a cationic com-

plex with three labile acetonitrile ligands, $[\text{Pd}(\text{Fmes})(\text{NCMe})_3]\text{BF}_4$, and its reactivity towards mono and bidentate ligands. The chemistry of cationic complexes containing labile ligands is a very active field, mainly due to the catalytic properties of many of these complexes in olefin polymerization processes [4]. Cationic palladium complexes containing the fluorinated aryl ring, C_6F_5 have also been used as insertion-triggered radical polymerization of norbornene and copolymerization of norbornene with simple olefins [5].

2. Results and discussion

2.1. Synthesis and characterization of $[\text{Pd}(\text{Fmes})(\text{NCMe})_3]\text{BF}_4$

The reaction of $[\text{Pd}(\mu\text{-Cl})(\text{Fmes})(\text{NCMe})_2]$ [3e] with TIBF_4 in a dichloromethane/acetonitrile mixture leads to

* Corresponding author.

E-mail address: espinet@qi.uva.es (P. Espinet).

the formation of $[\text{Pd}(\text{Fmes})(\text{NCMe})_3]\text{BF}_4$ (**1a**), which was isolated as a white solid in 92% yield (Scheme 1).

The $\nu(\text{C}\equiv\text{N})$ IR absorptions of MeCN in **1a** appear at 2343 and 2326 cm^{-1} . The ^{19}F NMR spectrum of **1a** in CDCl_3 shows one broad signal at -59.66 ppm for the two *ortho*- CF_3 groups and a singlet at -63.29 ppm for the *para*- CF_3 . Addition of MeCN causes the sharpening of the *ortho*- CF_3 signal, giving rise to a fine singlet, as in the typical pattern for Fmes complexes [3]. The ^1H NMR spectrum of **1a** in CDCl_3 at room temperature shows two sharp singlets (relative intensity 2:9) arising from the Fmes hydrogen atoms and the hydrogens of the three coordinated NCMe ligands. At 253 K the signal of the latter splits into two singlets (relative intensity 3:6). At this temperature the ^{19}F NMR spectrum also shows a sharpening of the *ortho*- CF_3 signal. Moreover, both in the ^1H NMR and ^{19}F NMR low temperature spectra a small amount of a minor complex, likely to be $[\text{Pd}(\text{Fmes})(\text{NCMe})_2(\text{OH}_2)]\text{BF}_4$ (**5a**) (see data in Section 4), is detected. These features suggest that the three acetonitrile ligands become equivalent through a associative displacement and exchange that is catalyzed by small amounts of water or, more efficiently, by added MeCN. With just traces of water in the medium the process is fast in the ^1H NMR time scale and in the exchange limit for the ^{19}F NMR time scale. The exchange can be frozen in the ^1H NMR time scale upon cooling at 253 K, and catalytically accelerated in the ^{19}F NMR time scale by free MeCN. Scheme 2 shows only the equilibrium between **1a** and **5a** where the MeCN *trans* to Fmes is replaced by an aqua ligand from traces of water present in CDCl_3 . For the equivalences observed the other two acetonitriles must also enter in the exchange process (for instance by Berry pseudo-rotation in the pentacoordinated intermediate produced during the associative substitution process). The lability of the MeCN ligand, and the easy formation of organometallic [6], and coordination palladium aqua complexes [7] is well documented.

All the attempts to isolate **5a** were unsuccessful, but other cationic complexes described below are also in equilibrium with their corresponding aqua complexes, and one of them could be fully characterized.

Since MeCN may be easily replaced by other ligands, complex **1a** is a good precursor for other cationic (fluoromesityl)palladium(II) complexes. We have shown before that, although dissociative substitutions seem to operate in bis(fluoromesityl)palladium(II) complexes [3f], associa-

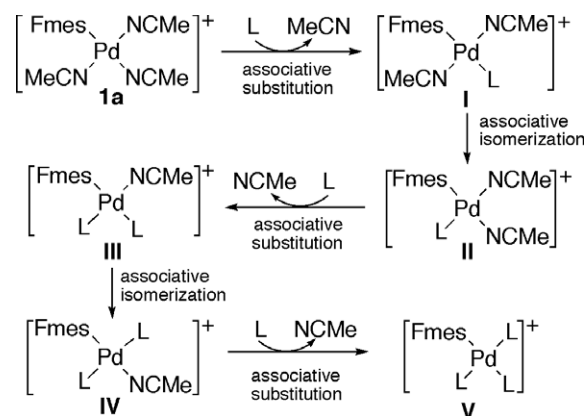
tive processes are preferred in mono(fluoromesityl)palladium(II) complexes [3e].

2.2. Reactivity of $[\text{Pd}(\text{Fmes})(\text{NCMe})_3]\text{BF}_4$ towards monodentate ligands

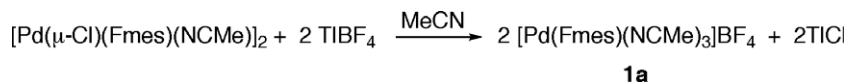
The monodentate ligands chosen to study the reactivity of **1a** were *t*-BuNC, different phenylphosphines as P-donors, and isomeric lutidines as N-donors. The latter offer the possibility of changing the ligand steric hindrance while keeping to a minimum the variation of donor ability.

According to the electronic *trans* effect and *trans* influence, the ligand exchange should operate as follows: The associative substitution should lead the incoming ligand to coordinate *trans* to Fmes, which is the group with the higher *trans* effect in **1a**. However, all the ligands used have a higher *trans* influence than MeCN (and lower than Fmes), which makes the initial kinetic product thermodynamically unstable, due to the highly destabilizing mutual *trans* influence of the incoming ligand and the Fmes group [8]. Therefore, a subsequent isomerization can be expected. If only electronic factors were considered and all reactions were fast, the successive substitution and isomerization reactions should follow the path proposed in Scheme 3.

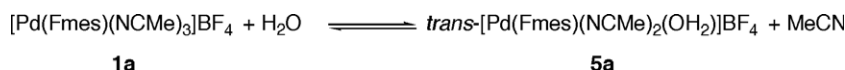
The experimental results found (Scheme 4) indicate that other factors must also be taken into account: (a) steric factors due to repulsion between ligands may be thermodynamically significant and may prevail over electronic factors in determining which isomer is the most stable



Scheme 3. Ideal sequential substitution/isomerization mechanism under electronic control in $[\text{Pd}(\text{Fmes})(\text{NCMe})_3]\text{BF}_4$ (**1a**).



Scheme 1. Synthesis of $[\text{Pd}(\text{Fmes})(\text{NCMe})_3]\text{BF}_4$ (**1a**).



Scheme 2. Process detected in the solutions of $[\text{Pd}(\text{Fmes})(\text{NCMe})_3]\text{BF}_4$ (**1a**).

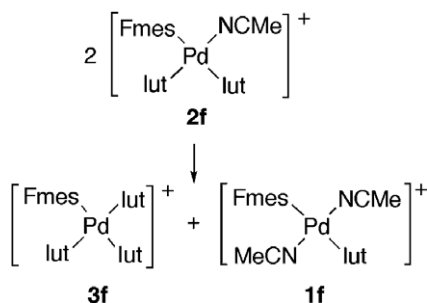
It should be noted that **2f** is the only disubstituted product with the incoming ligands coordinated mutually *cis* (**III** in Scheme 3) that has been isolated in the solid state (complexes **2b** (L = PPh₃) and **2i** (L = tht) could only be detected in solution). The NMR spectra show that **2f** is always accompanied with small amounts of **1f** and **3f** (Scheme 7), suggesting that this *cis* complex is unstable towards rearrangement.

The treatment of **1a** with the more hindered 2,4-lut in a 1:1 ratio at room temperature led to the monosubstituted product *trans*-[Pd(Fmes)(2,4-lut)(NCMe)₂]BF₄ (**3g**). When the reaction was carried out in refluxing CHCl₃ with a 4:1 excess of ligand, the trisubstituted product [Pd(Fmes)-(2,4-lut)₃]BF₄ (**1g**) was isolated. The disubstituted species could not be obtained. The addition of 2,6-lut (the most hindered lutidine) to **1a** only led to the monosubstituted product *trans*-[Pd(Fmes)(2,6-lut)(NCMe)₂]BF₄ (**3h**). Apparently, the high steric crowding in the axial positions of Pd precludes the formation of more substituted products.

The complex *trans*-[Pd(Fmes)(NCMe)(tht)₂]BF₄ (**2i**) (tht = tetrahydrothiophene) could be synthesized treating *trans*-[PdCl(Fmes)(tht)₂] [**3a**] with TIBF₄ in MeCN (Scheme 5). This reaction has to be carried out with excess of free tht in the reaction mixture, otherwise it leads to mixtures of **2i** and a new species. The latter could not be isolated pure, but the ¹H NMR spectrum shows two inequivalent NCMe ligands and one coordinated tht molecule (1:1:1) proving that it is the *cis* isomer of [Pd(Fmes)-(NCMe)₂(tht)]BF₄. The *ortho*-CF₃ groups of **2i** display a very broad signal in the ¹⁹F NMR spectrum in CDCl₃ at room temperature. This signal sharpens both in dry CDCl₃ and in wet CDCl₃. In the latter case, the MeCN signal appears broad and at chemical shifts near to that of free MeCN. These data point to an equilibrium between **2i** and the aqua complex *trans*-[Pd(Fmes)(OH₂)(tht)₂]BF₄ (**5i**), where a water molecule has replaced the MeCN ligand. In fact, complex **5i** was selectively obtained and isolated by refluxing **2i** in a THF/H₂O mixture (see Section 4).

2.3. Characterization of cationic complexes containing monodentate ligands

The ¹⁹F and ³¹P NMR spectra of all the complexes with phosphines are informative about the relative coordination of the Fmes group and phosphines. As reported for other



Scheme 7. Solution behavior of *cis*-[Pd(Fmes)(3,5-lut)₂(NCMe)]BF₄ (**2f**).

Fmes palladium(II) complexes, P–F coupling is observed when the Fmes group and the phosphines are coordinated *cis*, but not when these groups are mutually *trans* [3]. The ¹H NMR spectrum of **1d** could be interpreted only after a number of incoherent and selective ³¹P irradiation experiments.

The kind of phosphine used in **3c** can undergo the so-called “two-ring-flip mechanism”, [11] which exchanges the *exo*₂ and *exo*₃ conformers (two or three *ortho*-methyl groups in metal complexes of this kind of phosphine are oriented toward the metal atom). In the case of **3c** the ¹⁹F NMR spectrum at 213 K in CDCl₃ shows two non-equivalent *ortho*-CF₃ groups but one singlet in the ³¹P{¹H} NMR spectrum. This suggests that Pd–P rotation is slow at this temperature. The low temperature ¹H NMR spectrum shows a broad signal at 8.6 ppm, which is assigned to the H⁶ *endo* of the *exo*₂ conformer (in this conformation the *o*-methyl group is oriented away from the metal) [10]. This supports that the rotation around the P–C *ipso* bond, which exchanges the *exo*₂ and *exo*₃ conformers (where two or three *ortho*-methyl groups are oriented toward the metal atom), has also been arrested (in the NMR timescale) at this temperature. One of the conformers is clearly present in higher proportion, as observed also for neutral complexes [Pd(Fmes)XP(*o*-Tol)₃]₂ previously reported [3e].

The characterization of the lutidine complexes from their spectroscopic data is straightforward. An X-ray crystal structure analysis was carried out for the **3f**. A perspective view of the structure is given in Fig. 1, and selected distances and angles are listed in Table 1. The palladium atom is essentially square planar with minor distortions. The C–C–C angle at the *ipso* carbon atom of the Fmes

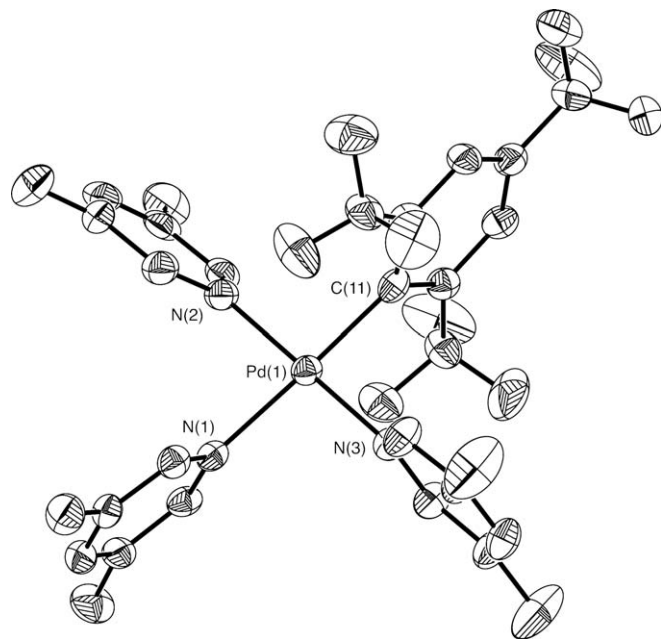


Fig. 1. ORTEP diagram of the cation [Pd(Fmes)(3,5-lut)₃]⁺ of **3f** showing the atom numbering scheme; the ellipsoids are drawn at 30% probability level.

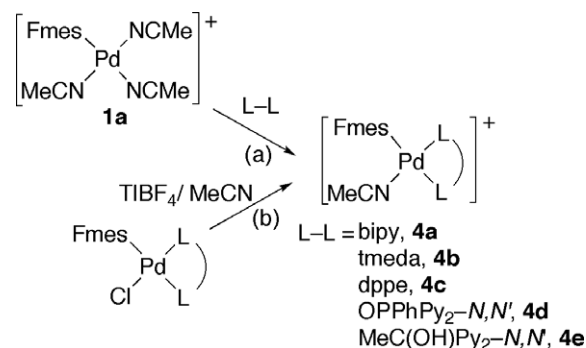
Pd(1)–C(11)	2.010(7)	N(3)–Pd(1)–N(1)	91.7(2)
Pd(1)–N(3)	2.035(5)	N(2)–Pd(1)–N(1)	87.7(2)
Pd(1)–N(2)	2.039(6)	N(3)–Pd(1)–N(2)	177.6(2)
Pd(1)–N(1)	2.103(6)	C(11)–Pd(1)–N(1)	177.9(2)
C(11)–Pd(1)–N(3)	90.4(2)	C(16)–C(11)–C(12)	113.8(7)
C(11)–Pd(1)–N(2)	90.2(2)		

group is significantly less than 120° [113.8(7)°], due to the electronic effects of the electropositive metal and electro-negative CF₃ substituents at these positions [12]. The Pd(1)–N(1) distance is larger than Pd(1)–N(3) or Pd(1)–N(2), due to the higher *trans* influence of the Fmes group compared to lutidine. The Fmes and two lutidine ligands are tilted in the same sense making angles of 86.5, 79 (N1, *trans* to Fmes), and 88° (N3, *cis* to Fmes) to the coordination plane. The other lutidine (N2, *cis* to the Fmes) is tilted also in the same sense making an angle of 65.1°. This torsion avoids the contact between one lutidine methyl group and one Fmes trifluoromethyl group of a neighboring cation in the crystal.

Low temperature NMR spectra of **1g** were needed in order to obtain additional information. The ¹⁹F NMR room temperature spectrum shows the presence of a major compound (91%) and two minor isomers [13]. Assuming that Fmes rotation is hindered due to its high steric requirements, restricted rotation of the 2,4-lut ligands around the Pd–N bonds will give rise to three atropisomers A–C in Fig. 2. The ¹H NMR spectrum of **1g** at 243 K clearly indicates that the major isomer observed corresponds to C, as the aromatic hydrogens and the methyl groups of the three lutidines are non-equivalent (see Section 4). C is the less hindered atropisomer, and therefore the most stable.

2.4. Synthesis and characterization of cationic complexes with bidentate ligands

Scheme 8 collects the complexes obtained with chelating ligands and their syntheses. The reactions of **1a** with differ-



Scheme 8. Syntheses of cationic complexes with bidentate ligands ((a) and (b) **4a**, **4b**; (a) **4c**, **4d**, **4e**).

ent bidentate ligands L–L in a 1:1 ratio lead to the cationic complexes [Pd(Fmes)(L–L)(NCMe)]BF₄ (L–L = bipy, **4a**; tmeda, **4b**; dppe, **4c**; OPPhPy₂–*N,N'*, **4d**; MeC(OH)Py₂–*N,N'*, **4e**) in high yields. All the reactions were fast, and no kinetic intermediates were detected. This is in contrast with the behavior observed in the analogous reaction of [Pd(μ-Cl)(Fmes)(NCMe)]₂ with dppe, which lead to kinetic and thermodynamic products, ([PdCl(Fmes)(NCMe)]₂(μ-dppe) and [PdCl(Fmes)(dppe)]), respectively [3e]. The alternative procedure treating the corresponding chloro-complexes [3a,3e] with TIBF₄ in MeCN, was also used to synthesize **4a** and **4b**.

The characterization of **4a**, **4b**, and **4c** from their spectroscopic data is straightforward. The chemical shift assigned to H⁶ in the complexes containing coordinated pyridyl groups (**4a**, **4d**, and **4e**) is clearly higher for the pyridyl moiety *cis* to NCMe. The same effect has been observed for the corresponding neutral chloro-complexes containing the same chelating ligands, although the shielding effect of the halogen is higher [3e].

One of the *ortho*-CF₃ groups in the complex [Pd(Fmes)(OPPhPy₂–*N,N'*)(NCMe)]BF₄ (**4d**) appears very upfield in the ¹⁹F NMR spectrum at room temperature, which can be attributed to the anisotropic shielding

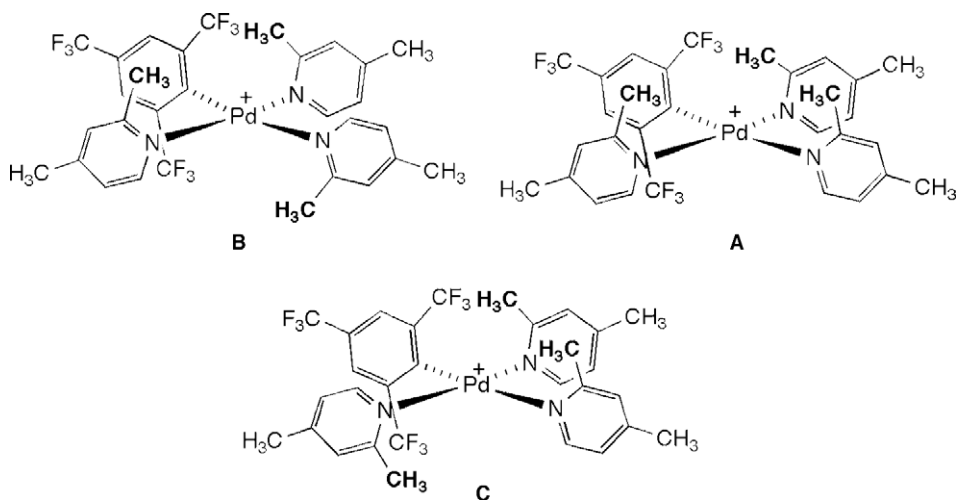


Fig. 2. Atropisomers in [Pd(Fmes)(2,4-lut)₃]BF₄ (**1g**).

produced by the phenyl group of the chelating ligand, as observed before for the analogous complexes $[\text{PdCl}(\text{Fmes})\text{-(OPhPy}_2\text{-}N,N')]$ [3e] and $[\text{PdBr}(\text{C}_6\text{F}_5)(\text{OPhPy}_2\text{-}N,N')]$ [14]. Moreover, both *ortho*-CF₃ groups give unusually broad signals, indicating that some dynamic process is occurring. The ¹H NMR spectrum of **4d** is as expected for the ligand chelated as N–N donor, but the signals of the two non-equivalent H³ atoms in the pyridyl groups are also broad. In a variable temperature study the H³ signals are well resolved pseudotriplets at 333 K and also at 213 K. These two protons remain non-equivalent at high temperatures, so an exchange process between both pyridyl groups can be discarded. A similar temperature effect is observed in the ¹⁹F NMR spectra in which at the *ortho*-CF₃ signals sharpen at 213 K without any appreciable change in their chemical shifts. The fluxional behavior of **4d** can be explained by the equilibrium depicted in Scheme 9 in which **4d** undergoes displacement of the nitrogen *trans* to Fmes (the most *trans* labilizing ligand) by an aqua ligand from traces of water, to give an aqua complex D in non-detectable amounts. The exchange rate is fast at high temperature, thus the signals from both the *ortho*-CF₃ and H³ atoms become sharp. When the temperature decreases, only the signals from **4d** are observable. The concentration of the putative aqua complex is very small, what makes the averaged chemical shift in the very uneven equilibrium almost identical to the chemical shift of very major component **4d**, recorded at low temperature.

Two conformers, (*endo*-CH₃) and (*endo*-OH), are plausible for **4e**. A single-crystal X-ray analysis was undertaken to establish which conformer is stable in the solid state. A perspective view of the cation $[\text{Pd}(\text{Fmes})\{(\text{OH})(\text{CH}_3)\text{-CPy}_2\text{-}N,N'\}(\text{NCMe})]^+$ is shown in Fig. 3. Selected bond lengths and angles are listed in Table 2. The square planar geometry of Pd is somewhat distorted towards tetrahedral, as previously observed for the neutral $[\text{PdCl}(\text{Fmes})\{(\text{OH})(\text{CH}_3)\text{-CPy}_2\text{-}N,N'\}]$ [3e]: N(2) is located 0.195(9) Å above the plane described by the Pd(1), C(11) and N(1) atoms, and N(3) is 0.209(9) Å below. This distortion is not as large as for *cis*-bis(fluoromesityl)palladium complexes in which the square-planar geometry is severely distorted [3f]. As usual, the C–C–C angle at the ipso carbon atom of the Fmes group is less than 120° [ca. 114.2(9)°] [12]. The Fmes ligand is nearly perpendicular to the coordination plane. The Pd···F₃C-*ortho* distances are longer than those found

in bis(fluoromesityl) complexes. Bonding Pd···F interactions can then be discarded, so the crowding in **4e** is responsible for the short non-bonding Pd···F contacts, as previously reported [3a]. The conformer found in the solid state has the methyl group of the (OH)(CH₃)CPy₂ ligand oriented towards the axial position of the coordination plane. The hydrogen atom of the OH group was located in a difference Fourier map and refined [15]. It is involved in O–H···F intermolecular contacts with the BF₄ counter-anion, with a rather short H(1)···F(12) distance of

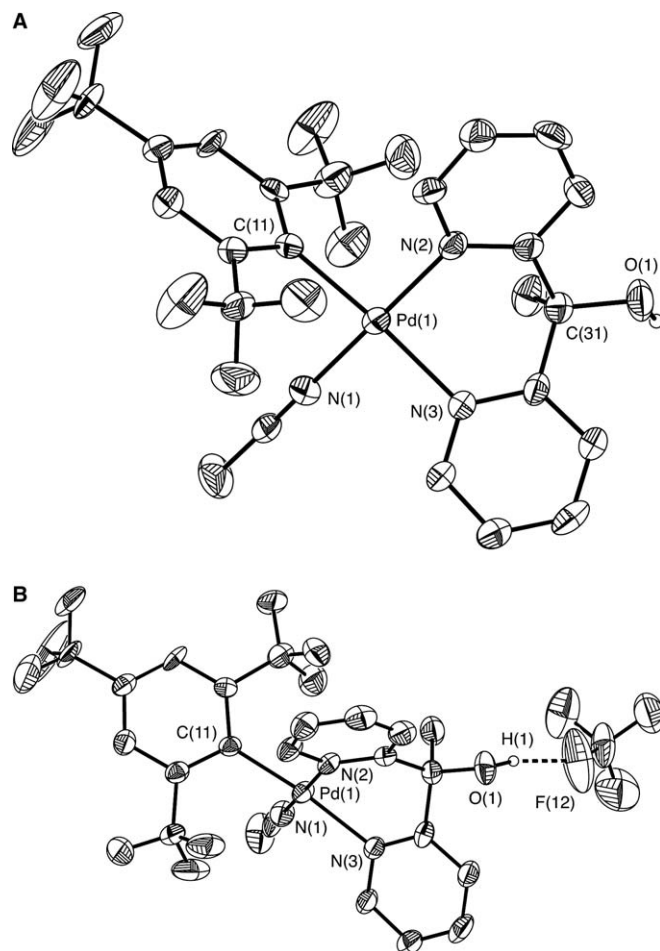
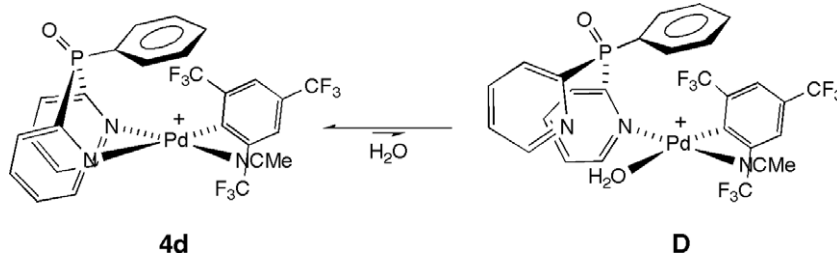


Fig. 3. Top: ORTEP diagram of the cation $[\text{Pd}(\text{Fmes})\{(\text{OH})(\text{CH}_3)\text{-CPy}_2\text{-}N,N'\}(\text{NCMe})]^+$ of **4e** showing the atom numbering scheme; the ellipsoids are drawn at 30% probability level. Bottom: Intermolecular H···F hydrogen bonds observed in **4e**.



Scheme 9. Water coordination in $[\text{Pd}(\text{Fmes})(\text{OPhPy}_2\text{-}N,N')(\text{NCMe})]\text{BF}_4$ (**4d**).

Table 2
Selected bond lengths (Å) and angles (°) for **4e**

Pd(1)–N(1)	1.973(9)	N(1)–Pd(1)–N(3)	92.4(3)
Pd(1)–C(11)	1.992(9)	N(2)–Pd(1)–N(3)	88.0(3)
Pd(1)–N(2)	2.029(8)	N(1)–Pd(1)–N(2)	174.5(4)
Pd(1)–N(3)	2.089(8)	C(11)–Pd(1)–N(3)	174.1(4)
N(1)–Pd(1)–C(11)	86.4(4)	C(16)–C(11)–C(12)	114.2(9)
C(11)–Pd(1)–N(2)	93.8(3)		

1.682(12) Å, and a O(1)–H(1)···F(12) angle of 158.5(4)°. Most H···F distances found in the Cambridge Data Base are within the range 1.73–2.5 Å, and only few are shorter than 1.7 Å, as in this case.

As observed for **1a** and **2i**, solutions of **4d** and **4e** also show equilibria with their respective aqua complexes [Pd(Fmes)(OH₂)(OPPhPy₂-*N,N'*)]BF₄ (**5d**) and [Pd(Fmes)(OH₂){(OH)(CH₃)CPy₂-*N,N'*}]BF₄ (**5e**) in wet deuterated solvents. The addition of water to **4d** and **4e** leads to observable amounts of the aqua complexes, which could not be isolated in the solid state. As for complexes **4**, the signal of H⁶ in aqua complexes containing coordinated pyridyl groups (**5a**, **5d**, and **5e**) appears clearly downfield for the pyridyl group *cis* to the aqua ligand. This shielding is lower than that observed for the acetonitrile complexes **4**, and much lower than for the corresponding neutral chloro-complexes containing the same chelating ligands [3e]. Therefore, the coordination-induced shift value for these ligands follows the sequence: Cl > NCMe > OH₂. The aqua complexes give back the acetonitrile complexes **4d** and **4e** upon addition of free MeCN.

3. Conclusions

Ligand substitution reactions at [Pd(Fmes)(NCMe)₃]BF₄ (**1a**) occur under mild conditions. A single Fmes group in a monoarylated complex can tilt and facilitate the approach of the incoming ligand, making associative substitutions a kinetically accessible pathway, at least for the first substitution. Subsequent substitutions can become more difficult depending on the ligands. The kinetic products of the initial substitution are consistent with the higher *trans* effect of the Fmes group. All the ligands used have higher *trans* effect than MeCN, what should make this kinetic product thermodynamically unstable towards isomerization, due to the tendency of Pd(II) to avoid ligands with high *trans* influence in mutually *trans* positions. However, the subsequent evolution of the reactions is not that simple, revealing that thermodynamic and kinetic steric effects also count and can prevail on the purely electronic predictions.

It is worth noting that in a number of cases H₂O, whether added or as adventitious water in the solvent, has been detected to replace other ligands in equilibrium, including chelating pyridyl ligands. This frequent occurrence suggests that the smaller size of the water molecule might also be a contribution to favor this otherwise unusual ligand competition.

4. Experimental

4.1. General comments

All reactions were carried out under an atmosphere of dry N₂, and at room temperature unless otherwise indicated. Solvents were purified according to standard procedures [16]. 1,3,5-C₆H₃(CF₃)₃ (FmesH) was purchased from Fluorochem, and Li(Fmes) was prepared as described in the literature [1a,16,17], and used immediately in situ without further purification. The chlorofluoromesityl complexes used as starting materials were prepared as previously described [3]. TIBF₄ was obtained as reported [18] (*Caution*. Ti(I) derivatives are toxic and should be handled with care).

Infrared spectra were recorded in a Perkin–Elmer 883 or 1720X apparatus as Nujol mulls between polystyrene films from 4000 to 200 cm⁻¹. Only the most significant absorptions are herein indicated for clarity (for the rest of IR absorptions see [Supplementary Material](#)). NMR spectra were recorded on Bruker AC-300 or ARX-300 instruments in dry CDCl₃ at room temperature unless otherwise stated. NMR spectra are referred to TMS, CFCl₃, or 85% aqueous H₃PO₄, coupling constants are measured in Hz, and *trans* and *cis* are referred to Fmes unless otherwise indicated. The signals in the ¹⁹F NMR assigned to ¹¹BF₄⁻ and ¹⁰BF₄⁻ appear within the range –153 to 154 ppm for all the complexes described ([Supplementary Material](#)). Elemental analyses were performed on a Perkin–Elmer 2400B micro-analyzer. Electrical conductivity measurements were carried out at room temperature with a Crison 522 conductimeter on ca. 5 × 10⁻⁴ M solutions; the range of molar conductivity for 1/1 electrolytes is 135–155 S cm² mol⁻¹ in acetonitrile solutions [19], although values of ca. 80 S cm² mol⁻¹ have been also described [20]. The molar conductivities of all the complexes herein described are in the range 94–115 S cm² mol⁻¹ ([Supplementary Material](#)).

4.2. [Pd(Fmes)(NCMe)₃]BF₄ (**1a**)

A 100 mL flask was successively charged with [Pd(μ-Cl)(Fmes)(NCMe)₂] [3e] (1.310 g, 1.42 mmol), MeCN (8 mL), CH₂Cl₂ (50 mL), and TIBF₄ (0.860 g, 2.98 mmol), and the mixture was stirred for 16 h. The solution was then filtered on dry Celite, the solvents were pumped off, and the residue was washed with Et₂O (3 × 10 mL), yielding 1.567 g (92%) of **1a** as an off-white solid. IR: 2343 s, 2326 vs, 2298 vs. ¹⁹F NMR (253 K) δ –59.60 (s, *ortho*-CF₃, 6F), –63.10 (s, *para*-CF₃, 3F). ¹H NMR (253 K) δ 7.86 (s, C₆H₂(CF₃)₃, 2H), 2.52 (s, *trans*-CH₃CN, 3H), 2.35 (s, *cis*-CH₃CN, 6H). Anal. Calc. for C₁₅H₁₁BF₁₃N₃Pd: C, 30.16; H, 1.86; N, 7.03. Found: C, 30.15; H, 1.93; N, 6.85%.

4.3. [Pd(Fmes)(PPh₂)₃]BF₄ (**1d**)

PPh₂ (0.074 g, 0.4 mmol) was added to a solution of **1a** (0.060 g, 0.1 mmol) in CH₂Cl₂ (10 mL), and the mixture was stirred for 1 h. The volatiles were pumped off, and the

residue was washed with Et₂O (3 × 10 mL), dried in vacuo, and stored under nitrogen, yielding 0.056 g (54%) of **1d** as a white solid. ¹⁹F NMR δ -59.60 (t, *J*_{PF} = 8.0, *ortho*-CF₃, 6F), -63.60 (s, *para*-CF₃, 3F). ³¹P{¹H} NMR δ 0.2 (dsept, ²*J*_{PP} = 34.0 (*cis*), *J*_{PF} = 8.0, *cis*-PPh₂, 2P), -8.4 (t, ²*J*_{PP} = 34.0, *trans*-PPh₂, 1P). ¹H {³¹P} NMR δ 7.20 (m, C₆H₅, 30H, and C₆H₂(CF₃)₃, 2H), 6.60 (s, *trans*-PPh₂, 1H), 6.15 (s, *cis*-PPh₂, 2H). ¹H NMR δ 7.20 (m, C₆H₅, 30H; C₆H₂(CF₃)₃, 2H), 6.60 (dt, ¹*J*_{PH} = 300.0, ³*J*_{PH} = 3.0, PPh₂ *trans*, 1H), 6.15 (AA'XX'M system, ¹*J*_{PH} = 377.0, ²*J*_{PP} = 357 (*trans*), ³*J*_{PH} = 8.0 (*cis*), ³*J*_{PH} = 7.0 (*trans*), PPh₂ *cis*, 2H). Anal. Calc. for C₄₅H₃₅BF₁₃P₃Pd: C, 52.33; H, 3.42. Found: C, 52.17; H, 3.45%.

4.4. [Pd(*Fmes*)(CN^{*t*}Bu)₃]BF₄ (**1e**)

CN^{*t*}Bu (0.028 g, 0.33 mmol) was added to a solution of **1a** (0.060 g, 0.1 mmol) in CH₂Cl₂ (10 mL), and the mixture was stirred for 8 h. Then Et₂O was added (ca. 10 mL) and the solution was cooled to -20 °C. The microcrystalline white solid obtained was filtered, washed with Et₂O (3 × 3 mL), and dried in vacuo, yielding 0.054 g (74%). IR (CH₂Cl₂): 2306 m, 2235 s. ¹⁹F NMR δ -61.30 (s, *ortho*-CF₃, 6F), -63.28 (s, *para*-CF₃, 3F). ¹H NMR δ 8.00 (s, C₆H₂(CF₃)₃, 2H), 1.69 (s, CNC₄H₉ *trans*, 9H), 1.41 (s, CNC₄H₉ *cis*, 18H). Anal. Calc. for C₂₄H₂₉BF₁₃N₃Pd: C, 39.83; H, 4.04; N, 5.81. Found: C, 39.85; H, 3.88; N, 5.79%.

4.5. *cis*-[Pd(*Fmes*)(3,5-*lut*)₃]BF₄ (**1f**)

A 100 mL flask was successively charged with **1a** (0.060 g, 0.1 mmol), CH₂Cl₂ (10 mL), and 3,5-lutidine (0.043 g, 0.4 mmol), and the mixture was stirred for 10 h. Work up as for **1e** yielded 0.061 g (77%). ¹⁹F NMR δ -58.10 (s, *ortho*-CF₃, 6F), -63.34 (s, *para*-CF₃, 3F). ¹H NMR δ 8.09 (s, NC₅H₃(CH₃)₂ *trans*, H², 2H), 7.99 (s, NC₅H₃(CH₃)₂ *cis*, H², 4H), 7.80 (s, C₆H₂(CF₃)₃, 2H), 7.53 (s, NC₅H₃(CH₃)₂ *trans*, H⁴, 1H), 7.41 (s, NC₅H₃(CH₃)₂ *cis*, H⁴, 2H), 2.32 (s, NC₅H₃(CH₃)₂ *trans*, 6H), 2.23 (s, NC₅H₃(CH₃)₂ *cis*, 12H). Anal. Calc. for C₃₀H₂₉BF₁₃N₃Pd: C, 45.28; H, 3.67; N, 5.28. Found: C, 45.19; H, 3.62; N, 5.46%.

4.6. [Pd(*Fmes*)(2,4-*lut*)₃]BF₄ (**1g**)

A 100 mL flask was successively charged with **1a** (0.060 g, 0.1 mmol), CHCl₃ (15 mL), and 2,4-lutidine (0.043 g, 0.4 mmol), and the mixture was refluxed for 22 h. Then the solution was filtered on dry Celite, Et₂O was added (ca. 15 mL) to the filtrate, and the solution was cooled to -20 °C. The microcrystalline white solid obtained was filtered, washed with Et₂O (3 × 3 mL), and dried in vacuo, yielding 0.040 g (51%). ¹⁹F NMR (243 K, atropisomer C) δ -58.37 (s, *ortho*-CF₃, 3F), -58.42 (s, *ortho*-CF₃, 3F), -63.17 (s, *para*-CF₃, 3F) (C: 91%). ¹⁹F NMR (298 K) δ -57.54 (br, *ortho*-CF₃, 6F, minor species), -58.23 (s, *ortho*-CF₃, 3F of isomer C), -58.31 (s, *ortho*-

CF₃, 3F of atropisomer C), -63.44 (s, *para*-CF₃, 3F of minor species). ¹⁹F NMR (333 K) δ -57.99 (br, *ortho*-CF₃, 6F all species), -63.63 (s, *para*-CF₃, 3F all species). ¹H NMR (243 K, atropisomer C) δ 8.21 (d, *J* = 6.0, NC₅H₃(CH₃)₂, H⁶, 1H), 8.09 (d, *J* = 6.0, NC₅H₃(CH₃)₂, H⁶, 1H), 7.84 (s, C₆H₂(CF₃)₃, 2H), 7.85 (d, *J* = 6.0, NC₅H₃(CH₃)₂, H⁶, 1H), 7.19 (s, NC₅H₃(CH₃)₂ *trans*, H³, 1H), 7.08 (s, NC₅H₃(CH₃)₂ *cis*, H³, 2H), 7.05 (d, *J* = 6.0, NC₅H₃(CH₃)₂, H⁵, 1H), 7.00 (d, *J* = 6.0, NC₅H₃(CH₃)₂, H⁵, 1H), 6.89 (d, *J* = 6.0, NC₅H₃(CH₃)₂, H⁵, 1H), 2.42 (s, NC₅H₃(CH₃)₂, 3H), 2.36 (s, NC₅H₃(CH₃)₂, 3H), 2.32 (s, NC₅H₃(CH₃)₂, 6H), 2.31 (s, NC₅H₃(CH₃)₂, 3H), 2.25 (s, NC₅H₃(CH₃)₂, 3H). ¹H NMR (298 K, atropisomer C) δ 8.24 (m, NC₅H₃(CH₃)₂, H⁶, 1H), 8.12 (m, NC₅H₃(CH₃)₂, H⁶, 1H), 7.91 (d, *J* = 6.0, H⁶, NC₅H₃(CH₃)₂, 1H), 7.83 (s, C₆H₂(CF₃)₃, 2H), 7.20 (s, H³, NC₅H₃(CH₃)₂ *trans*, 1H), 7.08 (m, NC₅H₃(CH₃)₂ and NC₅H₃(CH₃)₂, 3H), 6.97 (m, NC₅H₃(CH₃)₂, H⁵, 1H), 6.89 (m, NC₅H₃(CH₃)₂, H⁵, 1H), 2.44 (s, NC₅H₃(CH₃)₂, 3H), 2.36 (s, NC₅H₃(CH₃)₂, 3H), 2.33 (m, NC₅H₃(CH₃)₂, 12H). ¹H NMR (333 K, all species) δ 8.20 (s, NC₅H₃(CH₃)₂, H⁶, 2H), 7.99 (d, *J* = 6.0, NC₅H₃(CH₃)₂, H⁶, 1H), 7.82 (s, C₆H₂(CF₃)₃, 2H), 7.20 (s, NC₅H₃(CH₃)₂ *trans*, H³, 1H), 7.13 (d, *J* = 6.0, NC₅H₃(CH₃)₂, H⁵, 1H), 7.08 (s, NC₅H₃(CH₃)₂ *cis*, H³, 2H), 6.93 (br, NC₅H₃(CH₃)₂, H⁵, 2H), 2.42 (s, NC₅H₃(CH₃)₂, 6H), 2.38 (s, NC₅H₃(CH₃)₂, 6H), 2.33 (s, NC₅H₃(CH₃)₂, 6H). Anal. Calc. for C₃₀H₂₉BF₁₃N₃Pd: C, 45.28; H, 3.67; N, 5.28. Found: C, 44.94; H, 3.60; N, 5.27%.

4.7. *trans*-[Pd(*Fmes*)(NCMe)(PPh₃)₂]BF₄ (**2b**)

Method A. A 100 mL flask was successively charged with **1a** (0.060 g, 0.1 mmol), MeCN (10 mL), and PPh₃ (0.105 g, 0.4 mmol), and the mixture was refluxed for 16 h. Then the solution was filtered on dry Celite, and the volatiles were pumped off. The solid residue was crystallized in CH₂Cl₂-hexane at -20 °C, yielding a microcrystalline white solid, which was filtered, washed with cold hexane (3 × 3 mL), dried in vacuo, and stored under nitrogen. Yield: 0.061 g (59%). *Method B.* A 100 mL flask was successively charged with *trans*-[Pd(*Fmes*)Cl(PPh₃)₂] [**3a**] (0.095 g, 0.1 mmol), MeCN (10 mL), and TIBF₄ (0.032 g, 0.11 mmol), and the mixture was refluxed for 6 h. The volatiles were pumped off, CH₂Cl₂ (10 mL) was added to the residue, which was filtered on dry Celite. Then hexane was added (ca. 15 mL) and the solution was cooled to -20 °C, yielding 0.068 g (65%) of **2b**. IR: 2322 m, 2294 w. ¹⁹F NMR δ -58.59 (t, *J*_{PF} = 5.0, *ortho*-CF₃, 6F), -63.40 (s, *para*-CF₃, 3F). ³¹P{¹H} NMR δ 20.5 (sept, *J*_{PF} = 5.0). ¹H NMR δ 7.50 (m, C₆H₅, 30H), 7.28 (s, C₆H₂(CF₃)₃, 2H), 1.58 (t, *J*_{PH} = 1.0, CH₃CN, 3H). Anal. Calc. for C₄₇H₃₅BF₁₃NP₂Pd: C, 54.28; H, 3.39; N, 1.35. Found: C, 53.98; H, 3.58; N, 1.21%.

4.8. *cis*-[Pd(*Fmes*)(3,5-*lut*)₂(NCMe)]BF₄ (**2f**)

A 100 mL flask was successively charged with **1a** (0.060 g, 0.1 mmol), CH₂Cl₂ (10 mL), and 3,5-lutidine

(0.021 g, 0.2 mmol), and the mixture was stirred for 30 min. Work up as for **1e** yielded 0.032 g (44%) of **2f** as a white solid. IR: 2334 m, 2307 w. ^{19}F NMR δ -58.77 (s, *ortho*-CF₃, 6F), -63.26 (s, *para*-CF₃, 3F). ^1H NMR δ 8.15 (s, NC₅H₃(CH₃)₂ *trans*, H², 2H), 7.89 (s, NC₅H₃(CH₃)₂ *cis*, H², 2H), 7.86 (s, C₆H₂(CF₃)₃, 2H), 7.55 (s, NC₅H₃(CH₃)₂ *trans*, H⁴, 1H), 7.42 (s, NC₅H₃(CH₃)₂ *cis*, H⁴, 1H), 2.40 (s, NC₅H₃(CH₃)₂ *trans*, 6H), 2.30 (s, CH₃CN, 3H), 2.21 (s, NC₅H₃(CH₃)₂ *cis*, 6H). Anal. Calc. for C₂₅H₂₃BF₁₃-N₃Pd: C, 41.15; H, 3.18; N, 5.76. Found: C, 40.93; H, 3.05; N, 5.58%.

4.9. *trans*-[Pd(*Fmes*)(*NCMe*)(*tht*)₂]BF₄ (**2i**)

Tetrahydrothiophene (0.088 g, 1 mmol) and TIBF₄ (0.032 g, 0.11 mmol) were successively added to a solution of [Pd(*Fmes*)Cl(*tht*)₂] [**3a**] (0.060 g, 0.1 mmol) in MeCN (10 mL), and the mixture was refluxed for 15 h. Then the volatiles were pumped off and the residue was extracted with CH₂Cl₂ (20 mL) and filtered on dry Celite. The volatiles were pumped off again, and the solid residue was washed with Et₂O (3 × 10 mL), yielding 0.041 g (59%) of **2i** as a pale yellow solid. IR: 2328 m, 2300 m. ^{19}F NMR δ -60.05 (s, *ortho*-CF₃, 6F), -63.24 (s, *para*-CF₃, 3F). ^1H NMR δ 7.92 (s, C₆H₂(CF₃)₃, 2H), 2.96 (m, SC₄H₈, H_α, 4H), 2.53 (s, CH₃CN, 3H), 2.05 (m, SC₄H₈, H_β, 4H). Anal. Calc. for C₁₉H₂₁BF₁₃NP₂S₂: C, 32.99; H, 3.06; N, 2.02. Found: C, 32.85; H, 3.00; N, 1.73%.

4.10. *trans*-[Pd(*Fmes*)(*NCMe*)₂(*PPh*₃)]BF₄ (**3b**)

A 100 mL flask was successively charged with **1a** (0.090 g, 0.15 mmol), CH₂Cl₂ (15 mL), and PPh₃ (0.039 g, 0.15 mmol), and the mixture was stirred for 6 h. Work up as for **1e** yielded 0.110 g (89%). IR: 2343 m, 2332 m, 2315 m. ^{19}F NMR δ -59.26 (s, *ortho*-CF₃, 6F), -63.20 (s, *para*-CF₃, 3F). $^{31}\text{P}\{^1\text{H}\}$ NMR δ 19.5 (s). ^1H NMR δ 7.95 (d, $J_{\text{PH}} = 2.0$, C₆H₂(CF₃)₃, 2H), 7.60 (m, C₆H₅, 15H), 1.91 (d, $J_{\text{PH}} = 1.0$, CH₃CN, 6H). Anal. Calc. for C₃₁H₂₃BF₁₃N₂PPd: C, 45.48; H, 2.83; N, 3.42. Found: C, 45.45; H, 2.99; N, 3.35%.

4.11. *cis*-[Pd(*Fmes*)(*NCMe*)₂(*PPh*₃)]BF₄ (*cis*-**3b**)

Assigned signals: ^{19}F NMR δ -59.04 (*ortho*-CF₃, d, $J_{\text{PF}} = 3.8$ Hz) -63.40 (*para*-CF₃, s). $^{31}\text{P}\{^1\text{H}\}$ NMR δ 26.56, m.

4.12. *trans*-[Pd(*Fmes*)(*NCMe*)₂{*P(o-Tol)*₃}]BF₄ (**3c**)

A 100 mL flask was successively charged with **1a** (0.060 g, 0.1 mmol), CH₂Cl₂ (10 mL), and P(*o-Tol*)₃ (0.032 g, 0.1 mmol), and the mixture was stirred for 2 h. The volatiles were pumped off, and the residue was washed with hexane (3 × 10 mL), yielding 0.074 g (86%) of **2b** as a white solid which was stored under nitrogen. IR: 2334 m, 2308 m. ^{19}F NMR δ -59.19 (s, *ortho*-CF₃,

6F), -63.24 (s, *para*-CF₃, 3F). $^{31}\text{P}\{^1\text{H}\}$ NMR δ 14.5 (s). ^1H NMR δ 7.95 (d, $J_{\text{PH}} = 2.00$, C₆H₂(CF₃)₃, 2H), 7.68 (m, C₆H₄CH₃, 3H), 7.56 (m, C₆H₄CH₃, 3H), 7.39 (m, C₆H₄CH₃, 6H), 2.26 (s, C₆H₄CH₃, 9H), 1.91 (s, CH₃CN, 6H). ^{19}F NMR (213 K) δ -58.57 (s, *ortho*-CF₃, 3F), -59.78 (s, *ortho*-CF₃, 3F), -63.20 (s, *para*-CF₃, 3F). $^{31}\text{P}\{^1\text{H}\}$ NMR (213 K) δ 13.8 (s). ^1H NMR (213 K) δ 8.60 (br, C₆H₄CH₃, H⁶, 1H), 7.96 (d, $J_{\text{PH}} = 2.0$, C₆H₂(CF₃)₃, 2H), 7.32 (m, C₆H₄CH₃, 11H), 3.00 (br, C₆H₄CH₃, CH₃ *endo*, 3H), 1.94 (m, CH₃CN and C₆H₄CH₃, 12H). Anal. Calc. for C₃₄H₂₉BF₁₃N₂PPd: C, 47.44; H, 3.40; N, 3.25. Found: C, 47.50; H, 3.50; N, 3.05%.

4.13. *trans*-[Pd(*Fmes*)(3,5-*lut*)(*NCMe*)₂]BF₄ (**3f**)

A 100 mL flask was successively charged with **1a** (0.060 g, 0.1 mmol), CH₂Cl₂ (10 mL), and 3,5-lutidine (0.011 g, 0.1 mmol), and the mixture was stirred for 30 min. Work up as for **1e** yielded 0.042 g (63%). IR: 2339 s, 2311 m. ^{19}F NMR δ -59.43 (s, *ortho*-CF₃, 6F), -63.23 (s, *para*-CF₃, 3F). ^1H NMR δ 8.21 (s, NC₅H₃(CH₃)₂, H², 2H), 7.89 (s, C₆H₂(CF₃)₃, 2H), 7.58 (s, NC₅H₃(CH₃)₂, H⁴, 1H), 2.44 (s, NC₅H₃(CH₃)₂, 6H), 2.28 (s, CH₃CN, 6H). Anal. Calc. for C₂₀H₁₇BF₁₃N₃Pd: C, 36.20; H, 2.58; N, 6.33. Found: C, 35.98; H, 2.51; N, 6.25%.

4.14. *trans*-[Pd(*Fmes*)(2,4-*lut*)(*NCMe*)₂]BF₄ (**3g**)

A 100 mL flask was successively charged with **1a** (0.090 g, 0.15 mmol), CH₂Cl₂ (15 mL), and 2,4-lutidine (0.016 g, 0.15 mmol), and the mixture was stirred for 2 h. Work up as for **1e** yielded 0.048 g (48%). IR: 2337 s, 2310 vw. ^{19}F NMR δ -59.30 (s, *ortho*-CF₃, 6F), -63.23 (s, *para*-CF₃, 3F). ^1H NMR δ 8.50 (d, $J = 6.0$, NC₅H₃(CH₃)₂, H⁶, 1H), 7.91 (s, C₆H₂(CF₃)₃, 2H), 7.31 (s, NC₅H₃(CH₃)₂, H³, 1H), 7.28 (d, $J = 6.0$, NC₅H₃(CH₃)₂, H⁵, 1H), 2.99 (s, NC₅H₃(CH₃)₂, 3H), 2.43 (s, NC₅H₃(CH₃)₂, 3H), 2.24 (s, CH₃CN, 6H). Anal. Calc. for C₂₀H₁₇BF₁₃N₃Pd: C, 36.20; H, 2.58; N, 6.33. Found: C, 35.96; H, 2.41; N, 6.04%.

4.15. *trans*-[Pd(*Fmes*)(2,6-*lut*)(*NCMe*)₂]BF₄ (**3h**)

A 100 mL flask was successively charged with **1a** (0.090 g, 0.15 mmol), CH₂Cl₂ (15 mL), and 2,6-lutidine (0.016 g, 0.15 mmol), and the mixture was stirred for 6 h. The volatiles were pumped off, and the residue was washed with Et₂O (3 × 10 mL), yielding 0.067 g (67%) of **2e** as a white solid. IR: 2340 s, 2310 s. ^{19}F NMR δ -58.94 (s, *ortho*-CF₃, 6F), -63.24 (s, *para*-CF₃, 3F). ^1H NMR δ 7.94 (s, C₆H₂(CF₃)₃, 2H), 7.74 (t, $J = 8.0$, NC₅H₃(CH₃)₂, H³, 1H), 7.30 (d, $J = 8.0$, NC₅H₃(CH₃)₂, H⁴, 2H), 3.19 (s, NC₅H₃(CH₃)₂, 6H), 2.24 (s, CH₃CN, 6H). Anal. Calc. for C₂₀H₁₇BF₁₃N₃Pd: C, 36.20; H, 2.58; N, 6.33. Found: C, 36.12; H, 2.56; N, 6.24%.

4.16. $[Pd(Fmes)(bipy)(NCMe)]BF_4$ (**4a**)

Method A. 2,2'-Bipyridyl (0.017 g, 0.11 mmol) was added to a solution of **1a** (0.060 g, 0.1 mmol) in CH_2Cl_2 (10 mL), and the mixture was stirred for 30 min. Then hexane was added (ca. 10 mL) and the solution was concentrated in vacuo, and cooled to $-20^\circ C$. The microcrystalline white solid obtained was filtered, washed with hexane (3×5 mL), and dried in vacuo. Yield: 0.047 g (70%). **Method B.** A 100 mL flask was successively charged with $[Pd(Fmes)Cl(bipy)]$ [**3a**] (0.058 g, 0.1 mmol), MeCN (10 mL), and $TiBF_4$ (0.032 g, 0.11 mmol), and the mixture was refluxed for 45 min. The volatiles were pumped off, CH_2Cl_2 (10 mL) was added to the residue, which was filtered on dry Celite. Work up as before gave 0.037 g (55%) of **5b**. IR: 2333 w, 2307 w. ^{19}F NMR δ -60.03 (s, *ortho*- CF_3 , 6F), -63.17 (s, *para*- CF_3 , 3F). 1H NMR δ 8.97 (d, $J = 5.0$, C_5H_4N , H^6 *cis* to NCMe, 1H), 8.35 (d, $J = 8.0$, C_5H_4N , 1H), 8.25 (d, $J = 8.0$, C_5H_4N , 1H), 8.19 (td, $J = 8.0$ and 1.0, C_5H_4N , 1H), 8.12 (td, $J = 8.0$ and 1.0, C_5H_4N , 1H), 8.01 (s, $C_6H_2(CF_3)_3$, 2H), 7.95 (t, $J = 6.0$, C_5H_4N , 1H), 7.33 (t, $J = 6.0$, C_5H_4N , 1H), 7.23 (t, $J = 5.0$, C_5H_4N , 1H), 2.52 (s, CH_3CN , 3H). Anal. Calc. for $C_{21}H_{13}BF_{13}N_3Pd$: C, 37.56; H, 1.95; N, 6.26. Found: C, 37.38; H, 1.98; N, 5.93%.

4.17. $[Pd(Fmes)(NCMe)(tmeda)]BF_4$ (**4b**)

Method A. Tetramethylethylenediamine (0.006 g, 0.051 mmol) was added to a solution of **1a** (0.030 g, 0.05 mmol) in MeCN (10 mL), and the mixture was stirred for 3 h. The volatiles were pumped off and the white solid was washed with Et_2O (3×5 mL) and dried in vacuo. Yield: 0.047 g (70%). **Method B.** A 100 mL flask was successively charged with $[Pd(Fmes)Cl(tmeda)]$ [**3e**] (0.108 g, 0.2 mmol), MeCN (15 mL), and $TiBF_4$ (0.064 g, 0.22 mmol), and the mixture was refluxed for 24 h. The volatiles were pumped off, CH_2Cl_2 (20 mL) was added to the residue, which was filtered on dry Celite. Then Et_2O was added (ca. 20 mL) and the solution was cooled to $-20^\circ C$. The microcrystalline off-white solid obtained was filtered, washed with Et_2O (3×5 mL), and dried in vacuo. Yield: 0.103 g (82%). IR: 2333 m, 2307 w. ^{19}F NMR δ -58.17 (s, *ortho*- CF_3 , 6F), -63.30 (s, *para*- CF_3 , 3F). 1H NMR δ 7.87 (s, $C_6H_2(CF_3)_3$, 2H), 2.94 (m, NCH_2 , 2H), 2.88 (m, NCH_2 , 2H), 2.84 (s, NCH_3 , 6H), 2.37 (s, NCH_3 , 6H), 2.35 (s, CH_3CN , 3H). Anal. Calc. for $C_{17}H_{21}BF_{13}N_3Pd$: C, 32.33; H, 3.35; N, 6.65. Found: C, 32.02; H, 3.14; N, 6.45%.

4.18. $[Pd(Fmes)(NCMe)(dppe)]BF_4$ (**4c**)

1,2-Bis(diphenylphosphino)ethane (0.060 g, 0.15 mmol) was added to a solution of **1a** (0.090 g, 0.15 mmol) in MeCN (10 mL), and the mixture was stirred for 1 h. The solution was concentrated in vacuo to ca. 1–2 mL, and Et_2O was added to the residue until a white solid precipi-

tated. The mixture was cooled to $-20^\circ C$, and the solid was filtered, washed with Et_2O (3×5 mL), and dried in vacuo. Yield: 0.096 g (70%). IR: 2324 m, 2294 w. ^{19}F NMR δ -59.47 (t, $J_{PF} = 5.0$, *ortho*- CF_3 , 6F), -63.33 (s, *para*- CF_3 , 3F). $^{31}P\{^1H\}$ NMR δ 56.6 (dsept, $J_{PP} = 21.0$, $J_{PF} = 5.0$, P *cis*, 1P), 48.5 (d, $J_{PP} = 21.0$, P *trans*, 1P). 1H NMR δ 7.65 (m, C_6H_5 , 10H), 7.63 (d, $J_{PH} = 3.0$, $C_6H_2(CF_3)_3$, 2H), 7.37 (m, C_6H_5 , 2H), 7.15 (m, C_6H_5 , 8H), 3.00 (m, PCH_2 , 2H), 2.40 (m, PCH_2 , 2H), 2.14 (s, CH_3CN , 3H). Anal. Calc. for $C_{37}H_{29}BF_{13}NP_2Pd$: C, 48.63; H, 3.20; N, 1.53. Found: C, 48.37; H, 3.15; N, 1.20%.

4.19. $[Pd(Fmes)(NCMe)(OPPhPy_2-N,N')]BF_4$ (**4d**)

OPPhPy₂ (0.062 g, 0.22 mmol) were added to a solution of **1a** (0.119 g, 0.2 mmol) in CH_2Cl_2 (15 mL), and the solution was stirred for 1 h. Work up as for **1e** yielded 0.149 g (94%) of a beige solid. IR: 2334 m, 2315 w. ^{19}F NMR δ -58.63 (br, *ortho*- CF_3 , 3F), -63.20 (br, *ortho*- CF_3 , 3F), -63.31 (s, *para*- CF_3 , 3F). ^{19}F NMR (213 K) δ -58.69 (s, *ortho*- CF_3 , 3F), -62.84 (s, *ortho*- CF_3 , 3F), -63.45 (s, *para*- CF_3 , 3F). $^{31}P\{^1H\}$ NMR δ 21.5 (s). 1H NMR δ 9.36 (d, $J = 5.0$, C_5H_4N , H^6 *cis* to NCMe, 1H), 8.85 (br, C_5H_4N , H^3 , 1H), 8.49 (br, C_5H_4N , H^3 , 1H), 8.29 (m, C_5H_4N , H^4 , 1H), 8.18 (m, C_5H_4N , H^5 and H^6 , 2H), 8.02 (s, $C_6H_2(CF_3)_3$, 1H), 7.73 (m, C_5H_4N , H^4 , 6H), 7.67 (s, $C_6H_2(CF_3)_3$, 1H), 7.33 (m, C_5H_4N , H^5 , 1H), 2.39 (s, $NCCH_3$, 3H). Anal. Calc. for $C_{27}H_{18}BF_{13}N_3OPPd$: C, 40.76; H, 2.28; N, 5.28. Found: C, 40.52; H, 2.56; N, 4.85%.

4.20. $[Pd(Fmes)(NCMe)\{(OH)(CH_3)CPy_2-N,N'\}]BF_4$ (**4e**)

(OH)(CH₃)CPy₂ (0.022 g, 0.11 mmol) was added to a solution of **1a** (0.060 g, 0.1 mmol) in CH_2Cl_2 (10 mL) and the solution was stirred for 3 h. Then hexane was added (ca. 10 mL) and the solution was concentrated in vacuo, and cooled to $-20^\circ C$. The microcrystalline white solid obtained was filtered, washed with hexane (3×5 mL), and dried in vacuo, yielding 0.052 g of **4e** (73%). IR: 2340 m, 2313 m. ^{19}F NMR (Me_2CO-d_6) δ -57.71 (br, *ortho*- CF_3 , 3F), -59.30 (br, *ortho*- CF_3 , 3F), -62.09 (s, *para*- CF_3 , 3F). 1H NMR (Me_2CO-d_6) δ 9.09 (d, $J = 5.5$, C_5H_4N , H^6 *cis* to NCMe, 1H), 8.45 (d, $J = 8.0$, C_5H_4N , H^3 , 1H), 8.32 (d, $J = 4.0$, C_5H_4N , H^3 , 1H), 8.25 (m, H^4 and H^5 of C_5H_4N and $C_6H_2(CF_3)_3$, 3H), 8.06 (s, $C_6H_2(CF_3)_3$, 1H), 7.88 (d, $J = 5.5$, C_5H_4N , H^6 , 1H), 7.76 (dd, $J = 5.0$ and 9.5, C_5H_4N , H^4 , 1H), 7.30 (ddd, $J = 7.5$, 6.0 and 1.5, C_5H_4N , H^5 , 1H), 6.71 (s, *OH*, 1H) 3.00 (s, CH_3 , 3H), 2.57 (s, $NCCH_3$, 3H). Anal. Calc. for $C_{23}H_{17}BF_{13}N_3OPd$: C, 38.61; H, 2.39; N, 5.87. Found: C, 38.05; H, 2.40; N, 5.45%.

4.21. $[Pd(Fmes)(NCMe)_2(OH_2)]BF_4$ (**5a**)

Assigned signals: ^{19}F NMR (253 K) δ -59.75 (s, *ortho*- CF_3 , 6F), -63.00 (s, *para*- CF_3 , 3F). 1H NMR (253 K) δ 2.30 (s, H_2O).

4.22. $[Pd(Fmes)(OH_2)(OPPhPy_2-N,N')]BF_4$ (**5d**)

Assigned signals: ^{19}F NMR δ -58.55 (br, *ortho*- CF_3 , 3F), -62.89 (br, *ortho*- CF_3 , 3F), -63.23 (s, *para*- CF_3 , 3F). 1H NMR δ 9.17 (d, $J = 5.0$, C_5H_4N , H^6 *cis* to OH_2 , 1H), 7.89 (s, $C_6H_2(CF_3)_3$, 1H), 7.53 (s, $C_6H_2(CF_3)_3$, 1H), 7.33 (m, C_5H_4N , H^5 , 1H).

4.23. $[Pd(Fmes)(OH_2)\{(OH)(CH_3)CPy_2-N,N'\}]BF_4$ (**5e**)

Assigned signals: ^{19}F NMR (Me_2CO-d_6) δ -57.87 (s, *ortho*- CF_3 , 3F), -59.11 (s, *ortho*- CF_3 , 3F), -62.09 (s, *para*- CF_3 , 3F). 1H NMR (Me_2CO-d_6) δ 8.93 (d, $J = 5.5$, C_5H_4N , H^6 *cis* to OH_2 , 1H), 6.69 (s, COH, 1H), 3.07 (s, CH_3 , 3H).

4.24. *trans*- $[Pd(Fmes)(OH_2)(tht)_2]BF_4$ (**5i**)

A solution of **2i** (0.035 g, 0.05 mmol) in THF/ H_2O (10 mL, 1:1) was refluxed for 6 h. The solvents were then removed in vacuo and the residue was extracted with Et_2O (3×5 mL). The colorless solution was concentrated in vacuo, and cooled to -20 °C. The microcrystalline white solid obtained was filtered, washed with cold hexane (3×3 mL), and dried in vacuo, yielding 0.010 g (30%). ^{19}F NMR δ -60.11 (s, *ortho*- CF_3 , 6F), -63.22 (s, *para*- CF_3 , 3F). 1H NMR δ 7.89 (s, $C_6H_2(CF_3)_3$, 2H), 2.92 (m, SC_4H_8 , H_α , 8H), 2.24 (br, H_2O , 2H), 2.00 (m, SC_4H_8 , H_β , 8H).

4.24.1. Experimental procedure for X-ray crystallography

Suitable single crystals of **3f** and **4e** were grown by slow diffusion of a concentrated dichloromethane solution of the complex into diethylether at -20 °C and mounted in glass fibers, and diffraction measurements were made using a Bruker SMART CCD area-detector diffractometer with Mo $K\alpha$ radiation ($\lambda = 0.71073$ Å) [21]. Intensities were integrated from several series of exposures, each exposure covering 0.3° in ω , the total data set being a hemisphere [22]. Absorption corrections were applied, based on multiple and symmetry-equivalent measurements [23]. The structure was solved by direct methods and refined by least squares on weighted F^2 values for all reflections (see Table 3) [24]. All non-hydrogen atoms were assigned anisotropic displacement parameters and refined without positional constraints. Hydrogen atoms were taken into account at calculated positions and their positional parameters were refined. The hydrogen atom of the hydroxyl group was located in a difference Fourier map and refined. To correct the systematic shortening of O–H bonds measured by X-ray diffraction, the H atom position was normalized. An O–H distance of 0.967 Å was imposed, a value that has been observed in alcohols by neutron diffraction [15]. Refinement proceeded smoothly to give $R_1 = 0.0616$ for **3f** and $R_1 = 0.0471$ for **4e** based on the reflections with $I > 2\sigma(I)$. Complex neutral-atom scattering factors were used [25].

Table 3

Crystal data and structure refinement for **3f** and **4e**

	3f	4e
Empirical formula	$C_{30}H_{29}BF_{13}N_3Pd$	$C_{23}H_{17}BF_{13}N_3OPd$
Formula weight	795.77	715.61
Temperature (K)	298(2)	298(2)
Wavelength (Å)	0.71073	0.71073
Crystal system	Monoclinic	Triclinic
Space group	$P2(1)/n$	$P\bar{1}$
<i>a</i> (Å)	12.5397(17)	8.459(3)
<i>b</i> (Å)	16.121(2)	11.856(4)
<i>c</i> (Å)	16.559(2)	13.354(4)
α (°)	90	95.595(9)
β (°)	97.048(4)	91.412(9)
γ (°)	90	94.905(7)
<i>V</i> (Å ³)	3322.0(8)	1327.3(7)
<i>Z</i>	4	2
D_{calc} (g cm ⁻³)	1.591	1.791
Absorption coefficient (mm ⁻¹)	0.657	0.814
<i>F</i> (000)	1592	704
Crystal size (mm)	$0.09 \times 0.08 \times 0.08$	$0.07 \times 0.05 \times 0.01$
Θ Range for data collection	1.77 – 23.25°	1.53 – 23.40°
Reflections collected	15741	6347
Independent reflections	4762	3848
Absorption correction	SADABS	SADABS
Maximum and minimum transmission factor	1.000000 and 0.639593	1.000000 and 0.577003
Data/restraints/parameters	4762/0/439	3848/0/385
Goodness-of-fit on F^2	1.009	1.000
R_1 [$I > 2\sigma(I)$]	0.0471	0.0616
wR_2 (all data)	0.1300	0.1501

Crystallographic data (excluding structure factors) for the structures **3f** and **4e** reported in this paper have been deposited with the Cambridge Crystallographic Data Centre as Supplementary publication with the following deposition numbers: CCDC-294981, and CCDC-294982 for complexes **3f**, and **4e** respectively. Copies of the data can be obtained free of charge on application to the CCDC, 12 Union Road, Cambridge CB2 1EZ, UK, fax: (internat.) +44 1223 336 033, email: deposit@ccdc.cam.ac.uk.

Acknowledgments

Financial support by the Ministerio de Educación y Ciencia (Project CTQ2004-07667/BQU) and the Junta de Castilla y León (Project No. VA 060/04) is very gratefully acknowledged.

Appendix A. Supplementary data

Supplementary data associated with this article can be found, in the online version, at doi:10.1016/j.jorganchem.2006.05.039.

References

- [1] (a) F.T. Edlmann, Comments Inorg. Chem. 12 (1992) 259, and references therein; (b) R.D. Schuler, A.H. Cowley, D.A. Atwood, R.A. Jones, M.R. Bond, C.J. Carrano, J. Am. Chem. Soc. 115 (1993) 2070;

- (c) R.D. Schuller, H.S. Isom, A.H. Cowley, D.A. Atwood, R.A. Jones, F. Olbrich, S. Corbelin, R.J. Lagow, *Organometallics* 163 (1994) 4058.
- [2] (a) V.C. Gibson, C. Redshaw, L.J. Sequeira, K.B. Dillon, W. Clegg, M.R.J. Elsegood, *J. Chem. Soc., Chem. Commun.* (1996) 2151;
(b) K.B. Dillon, V.C. Gibson, J.A.K. Howard, C. Redshaw, L. Sequeira, J.W. Yao, *J. Organomet. Chem.* 528 (1997) 179;
(c) M. Belay, F.T. Edelmann, *J. Organomet. Chem.* 479 (1994) C21;
(d) P. Espinet, S. Martín-Barrios, F. Villafañe, P.G. Jones, *Organometallics* 19 (2000) 290.
- [3] (a) C. Bartolomé, P. Espinet, F. Villafañe, S. Giesa, A. Martín, A.G. Orpen, *Organometallics* 15 (1996) 2019;
(b) C. Bartolomé, R. de Blas, P. Espinet, J.M. Martín-Álvarez, F. Villafañe, *Angew. Chem., Int. Ed.* 40 (2001) 2521;
(c) C. Bartolomé, P. Espinet, L. Vicente, F. Villafañe, J.P.H. Charmant, A.G. Orpen, *Organometallics* 21 (2002) 3536;
(d) C. Bartolomé, P. Espinet, J.M. Martín-Álvarez, F. Villafañe, *Inorg. Chim. Acta* 347 (2003) 49;
(e) C. Bartolomé, P. Espinet, J.M. Martín-Álvarez, F. Villafañe, *Eur. J. Inorg. Chem.* (2003) 3127;
(f) C. Bartolomé, P. Espinet, J.M. Martín-Álvarez, F. Villafañe, *Eur. J. Inorg. Chem.* (2004) 2326.
- [4] (a) See, for example: A. Sen, T.W. Lai, R.R. Thomas, *J. Organomet. Chem.* 358 (1988) 567;
(b) A. Sen, Z. Jiang, *Organometallics* 12 (1993) 1406;
(c) L.K. Johnson, S. Mecking, M. Brookhart, *J. Am. Chem. Soc.* 118 (1996) 267;
(d) S.A. Svejda, M. Brookhart, *Organometallics* 18 (1999) 65.
- [5] R. López Fernández, PhD thesis, University of Valladolid, Spain, 2004.
- [6] J. Vicente, A. Arcas, *Coord. Chem. Rev.* 249 (2005) 1135.
- [7] (a) P. Leoni, M. Sommovigo, M. Pasquali, S. Midollini, D. Braga, P. Sabatino, *Organometallics* 10 (1991) 1038;
(b) P.J. Stang, D.H. Cao, G.T. Poulter, A.T. Arif, *Organometallics* 14 (1995) 1110;
(c) M. Akita, T. Miyaji, N. Muroga, C. Mock-Knoblach, W. Adam, S. Hikichi, Y. Moro-oka, *Inorg. Chem.* 39 (2000) 2096;
(d) M. Fuss, H.U. Siehl, B. Olenyuk, P.J. Stang, *Organometallics* 18 (1999) 758.
- [8] For the concepts of “antisymbiotic effect” and “transphobia” see, respectively: R.G. Pearson, *Inorg. Chem.* 12 (1973) 712;
J. Vicente, J.A. Abad, A.D. Frankland, M.C. Ramírez de Arellano, *Chem. Eur. J.* 5 (1999) 3066.
- [9] C.A. McAuliffe, in: G. Wilkinson, R.D. Gillard, J.A. McCleverty (Eds.), *Comprehensive Coordination Chemistry*, vol. 2, Pergamon, Oxford, 1987, p. 1012.
- [10] R.A. Widenhoefer, H.A. Zhong, S.L. Buchwald, *Organometallics* 15 (1996) 2745, and references therein.
- [11] (a) A.K. Colter, I.I. Schuster, R.J. Kurland, *J. Am. Chem. Soc.* 87 (1965) 2278;
(b) A.K. Colter, I.I. Schuster, R.J. Kurland, *J. Am. Chem. Soc.* 87 (1965) 2279.
- [12] (a) A. Domenicano, A. Vaciago, C.A. Coulson, *Acta Crystallogr. Sect. B* 31 (1975) 221;
(b) A. Domenicano, P. Mazzeo, A. Vaciago, *Tetrahedron Lett.* (1976) 1029;
(c) A. Domenicano, P. Murray-Rust, A. Vaciago, *Acta Crystallogr. Sect. B* 39 (1983) 457, and references therein;
(d) R. Norrestam, L. Schepper, *Acta Chem. Scand. Ser. A* 35 (1981) 91.
- [13] We are convinced that the minor signals (6%, 3%) correspond to the aqua complexes *cis* and *trans*-[Pd(Fmes)(OH₂)(lut)₂] formed by substitution of 2,4-lut with traces of water present in the solvent.
- [14] J.A. Casares, P. Espinet, J.M. Martínez-Illarduya, Y.-S. Lin, *Organometallics* 16 (1997) 770.
- [15] F.H. Allen, O. Kennard, D.G. Watson, L. Brammer, A.G. Orpen, R. Taylor, *J. Chem. Soc., Perkin Trans. 2* (1987) S1.
- [16] D.D. Perrin, W.L.F. Armarego, *Purification of Laboratory Chemicals*, third ed., Pergamon Press, Oxford, 1988.
- [17] M. Scholz, H.W. Roesky, D. Stalke, K. Keller, F.T. Edelmann, *J. Organomet. Chem.* 366 (1989) 73.
- [18] F.J. Arnáiz, *J. Chem. Educ.* 74 (1997) 1332.
- [19] W. Geary, *Coord. Chem. Rev.* 7 (1971) 81.
- [20] (a) T.D. Dubois, D.W. Meek, *Inorg. Chem.* 8 (1969) 146;
(b) R.L. Dutta, D.W. Meek, D.H. Busch, *Inorg. Chem.* 9 (1970) 1215.
- [21] SMART V5.051 Diffractometer Control Software, Bruker Analytical X-ray Instruments Inc., Madison, WI, 1998.
- [22] SAINT V6.02 Integration Software, Bruker Analytical X-ray Instruments Inc., Madison, WI, 1999.
- [23] G.M. Sheldrick, SADABS: A Program for Absorption Correction with the Siemens SMART System, University of Göttingen, Germany, 1996.
- [24] SHELXTL Program System Version 5.1; Bruker Analytical X-ray Instruments Inc., Madison, WI, 1998.
- [25] *International Tables for Crystallography*, vol. C. Kluwer, Dordrecht, 1992.